Revisiting the core dynamics in high-order harmonic generation using Bohmian trajectories

A. S. Sanz,[1,2] B. B. Augstein,[2] J. Wu,[2] and C. Figueira de Morisson Faria[2]

[1] *Instituto de Física Fundamental (IFF–CSIC), Serrano 123, 28006 Madrid, Spain*
[2] *Department of Physics and Astronomy, University College London, Gower Street, London WC1E 6BT, United Kingdom*

(Dated: January 11, 2013)

A full quantum model of high-order harmonic generation is presented from a Bohmian-mechanical perspective. According to the three-step model, this phenomenon occurs due to the laser-induced recombination of an electron ejected by tunnel ionization with its parent ion. However, when revisited within the Bohmian scenario, we find that the high-harmonic spectrum is generated by those trajectories that reside well inside the core rather than by those that undergo excursions out of it. This agrees with the outcome of the full solution of the time-dependent Schrödinger equation, in which the spectrum is obtained through the dipole acceleration. Furthermore, it shows that the innermost part of the core, represented by a single Bohmian trajectory, leads to the main contributions to the high-harmonic spectra. Nevertheless, one may relate time-frequency maps from these central Bohmian trajectories to classical electrons behaving according to the three-step model. This happens because the quantum phase carried by each Bohmian trajectory is influenced by the whole wavefunction and, therefore, also by those trajectories that leave the core.

PACS numbers: 32.80.Rm, 42.50.Hz, 42.65.Ky

High-order harmonic generation (HHG) is a very important phenomenon in strong-field physics [1–4], with a wide range of applications, such as subfemtosecond pulses [5–7], and the attosecond imaging of matter [8–10]. These applications are strongly based on the current paradigm for describing HHG: the three-step model (TSM) [11, 12]. According to the TSM, HHG takes place when an electron, initially ejected from the core by tunneling, comes back and recombines with its parent ion, emitting high-frequency radiation. This model, in both its classical [11] and quantum mechanical formulations, within the strong-field approximation (SFA) [12], has become a cornerstone for theoretical and experimental research on the subject. Furthermore, the physical picture of an electron returning to and recombining with the core has also been inferred from the direct solution of the time-dependent Schrödinger equation (TDSE). The HHG time profile, for high enough harmonic frequencies, coincides with the return times of a classical electron [13, 14].

It is also well established that "cleaner" HHG spectra, with a large plateau and a well-defined cutoff, are obtained from the expectation value of the dipole acceleration $\mathbf{a}(t) = \langle \Psi(t)| - \nabla V|\Psi(t)\rangle$, rather than from the dipole length in TDSE simulations [15, 16]. The dipole acceleration probes regions near the core, while the dipole length emphasizes regions closer to the integration boundaries [16]. This suggests that regions near the core, where the overlap between continuum and bound dynamics is likely to occur, are important to HHG. A legitimate questions is, however, whether one can single out a specific region in the core as being the most relevant to HHG. Apart from that, one may ask the question of how the above-stated overlap relates to the physical picture propagated by the TSM of an electron undergoing long excursions outside the core.

In this Letter we address these questions using Bohmian mechanics [17, 18], where well-defined trajectories can be assigned to quantum systems without violating any of the fundamental postulates and principles of standard quantum mechanics. This is possible because Bohmian trajectories contain quantum phase information, which classical trajectories do not. Furthermore, in contrast to other orbit-based approaches, such as the SFA [12], the influence of the binding potential is fully incorporated. Recently, Bohmian mechanics has been applied to strong-field physics at a descriptive and interpretational level [19–22] as well as a source for numerical algorithms [22, 23]. These works essentially follow the traditional scheme of considering a set of Bohmian trajectories and comparing their statistics with the corresponding quantum results. Here, on the contrary, we focus on the information obtained from the analysis of individual Bohmian trajectories showing that: (1) the HHG spectrum can be directly obtained from *a single* Bohmian trajectory (no statistics is needed), rather than from the dipole acceleration; (2) the specific trajectory that best reproduces the HHG spectrum remains in the core, instead of undergoing excursions out of this region; and (3) still, the physical picture related to the TSM can be extracted from the time profiles of the above-mentioned Bohmian trajectory. This shows that the innermost region of the core best reproduces the full HHG spectra.

Here, we employ a one-dimensional soft-core model, which suffices to illustrate the time-dependent electron dynamics, and yet contains the essential physical elements for linear polarization. Making use of the dipole approximation and the length gauge, the electron dynamics are described by the Hamiltonian (in atomic units) $H = -\frac{1}{2}\,\nabla^2 - \frac{1}{\sqrt{x^2+1}} - xE_0 f(t)$. The time dependence of the laser field is given by a flat-top function,

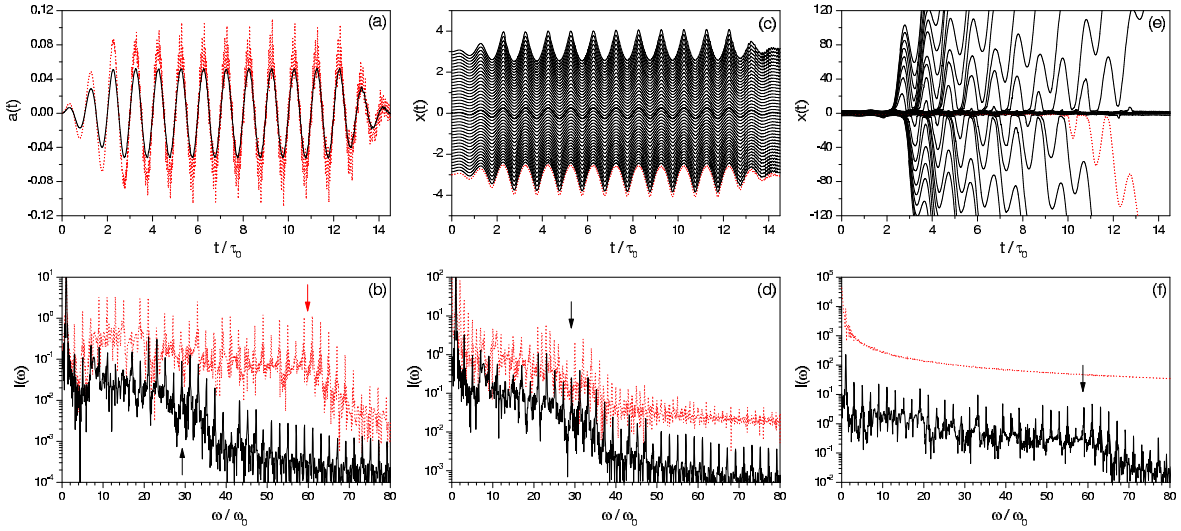

FIG. 1: Dipole acceleration (a) computed from the full TDSE solution and its frequency spectrum (b) for a pulse of frequency $\omega_0 = 0.05$ a.u. and field amplitudes $E_0 = 0.05$ a.u. (black solid line) and $E_0 = 0.085$ a.u. (red dotted line). The vertical arrows in the lower panels indicate the theoretically predicted positions of the cutoff frequencies, $\omega_c \approx 29.2\omega_0$ and $\omega_c \approx 59.2\omega_0$ for the lower and higher driving-field intensity, respectively. Set of 21 Bohmian trajectories for $E_0 = 0.05$ a.u. (c) and frequency spectrum (d) of those with initial positions at $x_1(0) = -3$ a.u. (red dotted line) and $x_{11}(0) = 0$ a.u. (black solid line). Set of 21 Bohmian trajectories for $E_0 = 0.085$ a.u. (e) and frequency spectrum (f) of those with initial positions at $x_9(0) = -0.6$ a.u. (red dotted line) and $x_{11}(0) = 0$ a.u. (black solid line).

$$f(t) = \begin{cases} (t/\tau_0)\sin(\omega_0 t), & 0 \le t < \tau_{\rm on} \\ \sin(\omega_0 t), & \tau_{\rm on} \le t < \tau_{\rm off} \\ [1-(t-\tau_{\rm off})/\tau_{\rm on}]\sin(\omega_0 t), & \tau_{\rm off} \le t \le \tau_f \end{cases} , \quad (1)$$

where ω_0 and $\tau_0 = 2\pi/\omega_0$ are the frequency and period of a field cycle, respectively. $\tau_{\rm on} = 2.25\,\tau_0$ is the time required for the external field to reach its maximum amplitude, $\tau_{\rm off} = 2.25\tau_0 + N\tau_0$ stands for the duration of the field with maximum amplitude, and $\tau_f = \tau_{\rm off} + 2.25\,\tau_0$ is the time at which the field is switched off (and our quantum simulations are completed). We have considered this particular type of pulse, with $N = 10$ ($\tau_f = 14.5\tau_0$), to ensure a high monochromaticity and therefore an optimal resolution of the HHG spectral features; as discussed elsewhere [24], other types of pulses, though more realistic, do not provide the same cleanliness for the same parameters used here. We assume that the system is initially in the ground state of the unperturbed soft-core potential, with energy $\epsilon_0 = -0.66978$ a.u. Following the usual scheme in Bohmian mechanics, first the wave function is expressed in polar form $\Psi(x,t) = \rho^{1/2}(x,t)\, e^{iS(x,t)/\hbar}$, with the probability density ρ and the phase S being real-valued functions of space and time. Then, the Bohmian trajectories are obtained [25] after integrating the (also real-valued) guidance equation $\dot{x} = \nabla S$ at each time-step, i.e., once $\Psi(x,t)$ is known. The latter is obtained by exactly solving the TDSE using the split operator method. A total of 21 initial conditions have been evenly chosen within the interval $x_0 \in [-x_c, x_c]$, with $x_c = 3$ a.u. In this way, the time evolution of most of the probability density will be well monitored, as the integrated probability for $|x| \ge x_c$ is only 0.41% of the total probability.

The dipole acceleration $a(t)$ and its power spectrum,

$$I(\omega) = \left| \int a(t)\, e^{-i\omega t} dt \right|^2 , \quad (2)$$

are displayed in Figs. 1(a) and (b), respectively, for two driving-field amplitudes. In both cases, the cutoff frequencies lie at $\omega_c \approx |\epsilon_0| + 3.17U_p$, where $U_p = E_0^2/4\omega_0^2$ is the ponderomotive energy, which agrees with the TSM. According to this model, the origin of these two HHG spectra is the same: the subsequent recombinations at the core ($x = 0$; $x \neq 0$ indicates the continuum, i.e., an unbound dynamics) of an electron that is ejected via tunneling and subsequently re-crosses $x = 0$ under the action of the external oscillating field. However, when the time evolution of the probability density is followed by Bohmian trajectories, which play the role of tracer particles [26], a very different picture emerges. In particular, the concept of tunneling itself, as such, does not exist in Bohmian mechanics: similarly to classical argumentations, only those trajectories with an appropriate initial energy/momentum are able to surmount the corresponding barrier; otherwise, the trajectories bounce backwards [27].

In panels (c) and (e) of Fig. 1, two subsets of 21 trajectories are displayed illustrating the flow of probability density. For low intensities, they follow back and forth the oscillations of the external field. In contrast, at higher intensities, while there is a subset of trajectories

that displays a similar behavior, part of the probability density is being ionized, with the corresponding trajectories eventually escaping from the core. In the TSM, the bound dynamics are restricted to $x = 0$. In the present model, however, these dynamics essentially seem to span the x values between the top of the narrowest effective potential barriers $V_{\rm eff}^{(\pm)}(x) = -1/\sqrt{x^2+1} \pm xE_0$. These boundaries correspond to the classical ionization points at maximum field, and occur at $x_m = \pm 4.299$ a.u. for $E_0 = 0.05$ a.u., and $x_m = \pm 3.198$ a.u. for $E_0 = 0.085$ a.u. Hence, by observing the probability flow, one may view the motion of the Bohmian trajectories oscillating around the initial position as "bound" [see panel (c)], while those undergoing excursions far away from their initial positions and eventually ionize irreversibly may be seen as "not bound" [see panel (e)]. This follows from the fact that Bohmian trajectories cannot cross through the same configuration space point at the same time [28].

Based on the above-mentioned criteria, we analyze the power spectrum associated with individual Bohmian trajectories, i.e., the spectrum obtained when the n-th Bohmian trajectory, $x_n(t)$, is substituted into Eq. (2) instead of $a(t)$. These spectra have been computed both for the lower- and the higher-intensity field [Figs. 1(d) and (f), respectively]. For the lower intensity, although the spectra in panel (d) refer to single trajectories, both contain information similar to that provided by the dipole acceleration [see panel (b)]. Furthermore, the spectra for trajectories $x_1(t)$ and $x_{11}(t)$ are very alike, because these trajectories display an analogous confined motion. However, notice that the closer the initial position of a trajectory is to $x = 0$, the more striking the similarity between the spectrum obtained for this specific trajectory and the dipole acceleration. For the innermost initial conditions, apart from the overall intensity, the spectral features of $a(t)$ and $x_{11}(t)$ are nearly identical. This seems rather counterintuitive, as (1) one would expect the spectrum to arise from the whole set of Bohmian trajectories (properly weighted), and (2), according to the TSM, the trajectories that leave from and return many times to the core should play a leading role.

For the higher-intensity field [Fig. 1(f)], the spectra of any ionizing trajectory look like that for $x_9(t)$, i.e., a continuous, monotonically decaying spectrum with no harmonic peaks, but only a small signature around the fundamental, $\omega = \omega_0$, and is thus very different from that provided by $a(t)$. At first glance, one would be tempted to associate these trajectories with the one described by the TSM, since the trajectory $x_9(t)$ undergoes two relatively long excursions out of the core before getting eventually ejected. However, once more, it is the innermost core trajectory that leads to the correct spectrum, as is observed from the analysis of $x_{11}(t)$. It is worth stressing that as the initial condition of the Bohmian trajectory gets further away from $x = 0$, not only does the power spectrum of the corresponding trajectory lose features of the correct HHG spectrum, but it also gains intensity. This is precisely the origin of the problems found when computing HHG spectra from the dipole length.

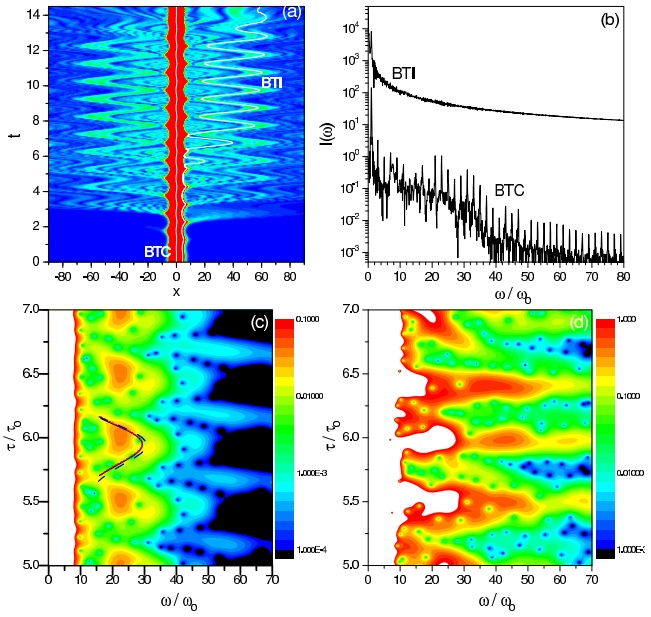

FIG. 2: (a) Time-evolution of the probability density for $E_0 = 0.05$ a.u. and two Bohmian trajectories launched from: $x = 0$ a.u. (BTC) and $x = 4.3125$ a.u. (BTI). (b) Power spectrum of the two Bohmian trajectories of panel (a). In (c) and (d), we display the time-frequency contour-plots for the Bohmian trajectories BTC and BTI, respectively, with a window function of width $\sigma_t = 10$ a.u. The superimposed lines in panel (c) give the classical returning times as a function of the electron kinetic energy upon return, for an electron ensemble in agreement with the TSM (red dotted line), with $x_0 = 0$ and $v_0 \neq 0$ (black solid line), and with $x_0 \neq 0$ and $v_0 = 0$ (blue dashed line). In the latter two cases the soft-core potential has been included. For details, see footnote [31].

Hence, the HHG spectrum is related to the phase information contained in the innermost part of the wave function, i.e., that which remains moving inside the core for longer times. This phase information, transmitted to the Bohmian trajectories through the above-mentioned guidance equation, allows us to monitor in an accurate fashion the evolution of the wave function [29] and therefore to reproduce the HHG spectrum, just as the dipole acceleration does [15].

Now, a legitimate question that arises after these results is: If HHG is described by Bohmian trajectories close to the core, why is the cutoff energy ω_c predicted by the TSM recovered? Time-frequency maps constitute a widespread tool employed to extract this type of information from TDSE computations [13, 30]. These maps are obtained through windowed Fourier transforms

$$I(\omega, t) = \int s(t)\, e^{-(t'-t)^2/\sigma_t^2} e^{-i\omega t'} dt', \qquad (3)$$

where $s(t)$ denotes the time-series to be analyzed. The Gaussian window function introduces time resolution, and allows us to blur up interference effects from the

spectrum, highlighting classical-like aspects that can be compared with the TSM. We have considered the lower field intensity case and two Bohmian trajectories: one that remains inside the core at any time (BTC) and another one (BTI) starting in the very-low probability region (beyond x_c), which eventually becomes ionized (such as in the high-intensity field case). These two trajectories, as well as a contour-plot of the probability density, are displayed in Fig. 2(a), and their spectra, which follow the same pattern described above, in Fig. 2(b). The time-frequency maps for these trajectories are shown in Figs. 2(c) and (d). The map for BTC follows a typically periodic structure, in accordance with the classical return times predicted by the TSM, while for BTI the map becomes very different [31]. Actually, when compared with the time-frequency map that one would obtain from the dipole acceleration, again we find that in the case of BTC the agreement is fairly good [as expected, since the topology of $a(t)$ and $x_{\rm BTC}(t)$ is essentially the same].

Summarizing, Bohmian trajectories show that the main contribution to the HHG spectrum arises from the most internal part of the wave function. It has been shown that a single Bohmian trajectory contains all the information necessary to obtain the HHG spectrum, namely the trajectory that starts at $x_0 = 0$ (and $\dot{x}_0 = \nabla S|_{t=0} = 0$), as in the case of the TSM. This is a much stronger statement than that provided by the dipole acceleration: By using the acceleration, one may conclude that the overlap between the continuum and bound part of the wavefunction near the core region are important. Here, we show that the part of the wavefunction located in the immediate vicinity of $x = 0$ provides the HHG spectrum. All other trajectories in the core region, when averaged out, contribute to blur up this contribution, thus giving rise to a difference in intensity between the spectra obtained from the trajectory starting at $x(0) = 0$ and from the dipole acceleration. We have chosen several driving-field intensities, frequencies, pulse shapes and binding potentials (not only those presented in this work) in order to corroborate that this applies to regimes with and without significant ionization. At first sight, one may have the impression that this contradicts the TSM. A deeper scrutiny, however, explains why the TSM works so well. The TSM reduces the influence of the core to a single point, i.e., $x = 0$. This is a good approximation, because the most relevant part of $\Psi(x,t)$ for HHG is strongly localized. Furthermore, quantum mechanically, one cannot attribute "bound" and "continuum" dynamics to well defined spatial regions. Hence, a Bohmian trajectory undergoing confined motion may contain both, as shown by the spectral and time-frequency analysis of $x_{11}(t)$. This is possible because this Bohmian trajectory evolves under the action of the wave function, which not only encompasses local information about the space variations of the potential function, but also about global changes of the quantum phase. This implies that the quantum mechanical phase associated with it is influenced by the *whole* wavefunction, i.e., also by the trajectories that ionize and return to the core. These latter trajectories, albeit related to a very low probability density, affect the quantum phase of the core trajectories according to the picture put across by the TSM. In contrast, a confined classical trajectory does not contain this phase information, and leads to very low electron kinetic energies. Hence, classical trajectories must revisit the core region recursively in order to probe the phase and provide us with the HHG spectrum.

This work was supported in part by the UK EPSRC, the CSC/BIS, the Ministerio de Economía y Competitividad (Spain) under Projects FIS2010-22082 and FIS2011-29596-C02-01, and the COST Action MP1006 (*Fundamental Problems in Quantum Physics*). A. S. Sanz would also like to thank the Ministerio de Economía y Competitividad for a "Ramón y Cajal" Research Grant and the University College London for its kind hospitality.

[1] T. Brabec and F. Krausz, Rev. Mod. Phys. **72**, 545 (2000).
[2] R. A. Ganeev, J. Phys. B **40**, R213 (2007).
[3] K. Midorikawa, Jpn. J. Appl. Phys. **50**, 090001 (2011).
[4] C. Altucci, J. W. G. Tisch, and R. Velotta, J. Mod. Opt. **58**, 1585 (2011).
[5] M. Hentschel *et al.*, Nature **414**, 509 (2001).
[6] R. Keinberger *et al.*, Nature **427**, 817 (2004).
[7] E. Goulielmakis *et al.*, Science **320**, 1614 (2008).
[8] J. Itatani *et al.*, Nature **432**, 867 (2004).
[9] O. Smirnova *et al.*, Nature **460**, 972 (2009).
[10] C. Vozzi *et al.*, Nat. Phys. **7**, 822 (2011).
[11] K. C. Kulander *et al.*, Phys. Rev. Lett. **70**, 1599 (1993); P. B. Corkum, Phys. Rev. Lett. **71**, 1994 (1993).
[12] M. Lewenstein *et al.*, Phys. Rev. A **49**, 2117 (1994).
[13] C. Figueira de Morisson Faria, M. Dörr, and W. Sandner, Phys. Rev. A **55**, 3961 (1997).
[14] Other physical mechanisms may also lead to HHG, such as continuum wave-packet interference, transitions involving bound states, or the recollision of two free electrons after laser-induced double-ionization. These mechanisms, however, either yield very small effects or are only relevant for much higher driving-field intensities. For details see, e.g., M. C. Kohler *et. al.*, Phys. Rev. Lett. **105**, 203902 (2010)), S. X. Hu *et. al.*, Phys. Rev. A **63**, 011403 (2001), or P. Koval *et. al.*, Phys. Rev. Lett. **98**, 043904 (2007), respectively.
[15] K. Burnett, V. C. Reed, J. Cooper, and P. L. Knight, Phys. Rev. A **45**, 3347 (1992).
[16] J. L. Krause, K. J. Schafer, and K. C. Kulander, Phys. Rev. A **45**, 4998 (1992)
[17] D. Bohm, Phys. Rev. **85**, 166 (1952); ibid. 180 (1952).
[18] P. R. Holland, *The Quantum Theory of Motion* (Cambridge University Press, Cambridge, 1993).
[19] X. Y. Lai, Q. Y. Cai, and M. S. Zhan, Eur. Phys. J. D **53**, 393 (2009); New J. Phys. **11**, 113035 (2009); Chin.

Phys. B **19**, 020302 (2010).
[20] P. Botheron and B. Pons, Phys. Rev. A **83**, 062704 (2011).
[21] N. Takemoto and A. Becker, J. Chem. Phys. **134**, 074309 (2011).
[22] A. Picón *et al.*, New J. Phys **12**, 083053 (2010).
[23] P. Botheron and B. Pons, Phys. Rev. A **82**, 021404R (2010).
[24] J. Wu, A. S. Sanz, B. B. Augstein, and C. Figueira de Morisson Faria (submitted for publication), pre-print arXiv:1301.1916
[25] One can also proceed the other way around, i.e., devising numerical methodology aimed at directly obtaining the Bohmian trajectories, from which relevant information about the quantum system is extracted, as done with the so-called *quantum trajectory methods* [e.g., see: R.E. Wyatt, *Quantum Dynamics with Trajectories* (Springer, New York, 2005)].
[26] A. S. Sanz and S. Miret-Artés, Am. J. Phys. **80**, 525 (2012).
[27] C. Dewdney and B. Hiley, Found. Phys. **12**, 27 (1982); C. Lopreore and R.E. Wyatt, Phys. Rev. Lett. **82**, 5190 (1999); A.S. Sanz and S. Miret-Artés, J. Phys. A **44**, 485301 (2011).
[28] A. S. Sanz and S. Miret-Artés, J. Phys. A: Math. Theor. **41**, 435303 (2008).
[29] A. S. Sanz, J. Phys. A: Math. Theor. **38**, 6037 (2005).
[30] S. Mallat, *A Wavelet Tour of Signal Processing* (Academic Press, London,1998).
[31] These return-time curves have been obtained for a classical electron ensemble by varying their ionization times within half a cycle of the driving field, both in the presence and in the absence of the soft-core potential. When the potential was absent, we assumed the initial position and velocities to be $x_0 = v_0 = 0$, in accordance with the TSM. When it was included, we either considered $x_0 = 0$ and a nonvanishing classical escape velocity $v_0 = \sqrt{2}$, or $v_0 = 0$ and a classical turning point $-x_0/[x_0^2 + 1]^{3/2} - E(t) = 0$. An important issue is that, in order to obtain classical kinetic energies in agreement with the time profile in Fig. 2, it was essential to induce an *unbound* motion in the electron ensemble, as suggested by the TSM.